

Ancestral chemotypes of cultivated grapevine with resistance to Botryosphaeriaceae-related dieback allocate metabolism towards bioactive stilbenes

Islam M. Khattab^{1,2} , Vaidurya P. Sahi¹ , Raymonde Baltenweck³ , Alessandra Maia-Grondard³ , Philippe Hugueney³ , Eva Bieler⁴, Markus Dürrenberger⁴ , Michael Riemann¹  and Peter Nick¹ 

¹Molecular Cell Biology, Botanical Institute, Karlsruhe Institute of Technology, Fritz-Haber-Weg 4, Karlsruhe 76131, Germany; ²Department of Horticulture, Faculty of Agriculture, Damanhour University, PO Box 59, Damanhour, Egypt; ³INRAE, SVQV UMR-A 1131, Université de Strasbourg, Colmar F-68000, France; ⁴Swiss Nanoscience Institute – Nano Imaging Lab, University of Basel, Klingelbergstrasse 50/70, Basel CH-4056, Switzerland

Summary

Author for correspondence:

Islam M. Khattab

Email: islam.khattab@agr.dmu.edu.eg

Received: 21 April 2020

Accepted: 24 August 2020

New Phytologist (2020)

doi: 10.1111/nph.16919

Key words: *Neofusicoccum parvum*, phenylpropanoid pathway, piceid chemotype, resveratrol-viniferin chemotype, *Vitis* resistance.

- Grapevine trunk diseases have devastating consequences on vineyards worldwide. European wild grapevines (*Vitis vinifera* subs. *sylvestris*) from the last viable population in Germany along the Rhine river showed variable degrees of resistance against *Neofusicoccum parvum* (strain Bt-67), a fungus associated with Botryosphaeriaceae-related dieback.
- Representative genotypes from different subclades of this population were mapped with respect to their ability to induce wood necrosis, as well as their defence responses in a controlled inoculation system.
- The difference in colonization patterns could be confirmed by cryo-scanning electron microscopy, while there was no relationship between vessel diameter and infection success. Resistant lines accumulated more stilbenes, that were in addition significantly partitioned to nonglycosylated viniferin trimers. By contrast, the susceptible genotypes accumulated less stilbenes with a significantly higher proportion of glycosylated piceid.
- We suggest a model in which in the resistant genotypes phenylpropanoid metabolism is channelled rapidly and specifically to the bioactive stilbenes. Our study specifies a resistant chemotype against grapevines trunk diseases and paves a way to breed for resistance against grapevine Botryosphaeriaceae-related dieback.

Introduction

Grapevine trunk diseases (GTDs), especially Botryosphaeriaceae-related dieback, have increasingly become a serious challenge recently, and are classified as one of the most devastating diseases threatening vineyards worldwide (Guan *et al.*, 2016; Spagnolo *et al.*, 2017). While these fungi are widespread in grapevine trunks without causing symptoms, the incidence of disease outbreaks has increased as a consequence of climate change, and there has been an increase in disease outbreaks for the family Botryosphaeriaceae in all woody plants (for reviews see Coakley *et al.*, 1999; Slippers & Wingfield, 2007). The classical approach to plant protection to such challenges is to kill potential pathogens by toxic chemicals. In the case of GTDs, this was achieved in the past by using arsenite, a practice that has been banned in Europe (European Commission, 2009). This approach not only leaves a negative ecological footprint but is also inappropriate for a pathogen that does not meet the Koch postulates, because it is present in healthy hosts that are symptom-free. Because conventional fungicides fail to control such

diseases (Wagschal *et al.*, 2008), most viticulturists root out the infected plants. Alternatively, they use stringent pruning to rejuvenate the trunk, but this lengthy process needs 3–5 yr to be completed. Hence the different forms of GTDs, such as Eutypa dieback, Esca syndrome and Botryosphaeriaceae-related dieback cause progressive economic damage of >US\$1140 million per year globally (Sosnowski *et al.*, 2008; Romanazzi *et al.*, 2009; Fontaine *et al.*, 2016).

GTDs are very complex syndromes that are hard to understand because the development of symptoms is not predictable and seems to depend on the condition of the host. For instance, members of the family Botryosphaeriaceae behave as endophytes (Slippers & Wingfield, 2007), colonizing the grapevine trunk through pruning wounds, and subsequently living during a latent, peaceful, phase without visible symptoms, often for years (Djoukeng *et al.*, 2009). Under conditions that are not fully understood, possibly when the host experiences severe stress conditions, the hitherto harmless endophyte switches to active pathogenicity culminating in rapid killing of the host (Slippers & Wingfield, 2007).

To what extent the virulence of Botryosphaeriaceae members becomes manifest as dieback, differs for different genera within this family. Symptoms can be severe as with the genus *Neofusicoccum*, moderate as in the sister genus *Diplodia*, or very mild as for the genus *Dothiorella* (Úrbez-Torres, 2011). The complexity of Botryosphaeriaceae-related dieback is extended even further by synergistic interactions among GTD pathogens. For instance, *Phaeoconiella chlamydospora* can evoke severe symptoms, if combined with other species from the Botryosphaeriaceae or with *Phaeoconiella aleophilum* (Úrbez-Torres *et al.*, 2013; Pierron *et al.*, 2016). The impact is substantial: 21 fungal species belonging to the family Botryosphaeriaceae have been reported to cause conspicuous economic losses in viticulture (Bertsch *et al.*, 2013).

Anatomical investigations at the infected internodes of grapevines have shown that the fungal hyphae colonize the xylem vessels, fibres and parenchyma rays, which holds true for several dieback diseases, as well as for Esca disease (Pouzoulet *et al.*, 2013; Gómez *et al.*, 2016). The finding that the susceptibility of different genotypes to GTDs shows considerable variability (Pierron *et al.*, 2016; Guan *et al.*, 2016) indicates that the spread of the mycelium in the infected stem can be contained by defence mechanisms of the host.

Unlike mammals, plants use an innate immunity composed of two layers: a broad-band so-called pathogen-associated molecular patterns (PAMP)-triggered immunity, PTI, is activated by cell surface-localized pattern recognition receptors (PRRs) directed against generic pathogen molecules, such as flagellin (bacteria) or chitin (fungi). These can be accompanied by nonproteinaceous components of the cell wall, and also those produced as a consequence of pathogen-inflicted damage, as emphasized by the invasion pattern model (Stael *et al.*, 2015; Schellenberger *et al.*, 2019). A second layer is a pathogen (often even strain)-specific effector-triggered immunity (ETI), activated in response to effectors that are secreted by the pathogen to quell PTI (Jones & Dangl, 2006; Schellenberger *et al.*, 2019).

In *Botryosphaeria* (Slippers & Wingfield, 2007), the cell wall acts as a site of host–pathogen signalling. It is relevant to note that PTI was shown to be linked to changes of cell wall composition: impaired PTI can be associated with enhanced lignification (Bacete *et al.*, 2018). In grapevines, the accumulation of stilbene phytoalexins is a central element of PTI against the oomycete *Plasmopara viticola*, and ascomycete *Erysiphe necator* (Pezet *et al.*, 2004; Jiao *et al.*, 2016). Due to this broad spectrum of targets, the stilbene pathway might also play a defensive role against Botryosphaeriaceae. This assumption is supported by comparative *in vivo* infection studies using *Neofusicoccum parvum*, a model species to study the dieback caused by members of the family Botryosphaeriaceae in grapevines. Here, phytoalexin genes and also the stilbene metabolites were found to accumulate in response to infection (Guan *et al.*, 2016; Massonnet *et al.*, 2017; Spagnolo *et al.*, 2017). In fact, the antifungal activity of resveratrol and δ -viniferin could be shown *in vitro* using three fungal strains associated with symptom expression (Stempien *et al.*, 2017). Among the tested strains, *Neofusicoccum parvum* Bt-67 was not only the most aggressive strain *in planta* (Guan *et al.*, 2016), but also the strain least affected

by stilbenes (Stempien *et al.*, 2017). Consequently, for our study, we selected *Neofusicoccum parvum* Bt-67 as a representative strain model to screen the resistance of *Vitis sylvestris* individuals towards Botryosphaeriaceae-associated dieback.

In the present study, we tested whether genetic differences in the inducibility of stilbenes contribute to the (observed) genetic differences in resistance to Botryosphaeriaceae. To address this, two preconditions have to be met: one needs a set of genotypes that contrast with respect to stilbene inducibility; and these genotypes have to be closely related to minimize the nonpathogen-related effects of genetic background. This was achieved using the *V. sylvestris* germplasm collection established in the Botanical Garden of the Karlsruhe Institute of Technology (KIT). The original purpose of this collection had been to rescue this highly endangered species from extinction by replicating the complete genetic diversity still available in Germany for this wild ancestor of domesticated grapevine (*Vitis vinifera* L. ssp. *vinifera*). Later, this germplasm was found to harbour numerous resilience factors against various diseases (Schröder *et al.*, 2015), cold stress (Wang *et al.*, 2019) and two species of the Botryosphaeriaceae (Guan *et al.*, 2016). Disease resistance cannot be understood in terms of a gene-for-gene concept, because most of these diseases had been introduced to Europe only in the 19th century, such that there is no co-evolutionary history. Instead, this ancestral grape population harbours factors contributing to a broad-band basal immunity (Duan *et al.*, 2015, 2016). Because domesticated grapevine (*V. vinifera* L. ssp. *vinifera*) has undergone several events of introgression by ssp. *sylvestris* during its spread in the Mediterranean (Arroyo-García *et al.*, 2006), some of these factors might still be found in autochthonous varieties.

This population harbours considerable genetic variability, also in comparison with other European populations of *V. sylvestris*, as assessed from molecular phylogeny using simple sequence repeat (SSR) markers (Nick, 2014). In particular, stilbene inducibility and speciation, assessed as metabolic response to a UV pulse, occurred in the form of two chemotypes (Duan *et al.*, 2015): the piceid chemotype (PC) accumulated only low amounts of stilbenes in the form of the biologically inactive glycoside, while the resveratrol-viniferin chemotype (RVC) accumulated high amounts of stilbenes in the form of the biologically active aglycon *trans*-resveratrol and its oligomers, viniferins, and exhibited elevated resistance to *Plasmopara viticola*. A large part of the collection was fully sequenced (Liang *et al.*, 2019). Our hypothesis leads to the implication that the RVC genotypes are more resistant to Botryosphaeriaceae infection (using controlled inoculation with *Neofusicoccum parvum* Bt-67) than the PC genotypes. We tested this by comparatively following colonization (to assess susceptibility), but also cellular and molecular aspects of colonization and host response in contrasting sets of PC and RVC.

Materials and Methods

Phylogenetic analysis based on genome-wide SNPs

Based on the full nuclear genomes from 89 genotypes including European varieties of *V. vinifera* varieties, wild Asian and

American species, and a collection of European Wild Grapes (*V. vinifera* spp. *sylvestris*) (Liang *et al.*, 2019) a database was constructed, using as reference genome from Pinot Noir clone PN40024 (<http://www.genoscope.cns.fr/externe/GenomeBrowse/r/Vitis/>). The BWA software was used for mapping paired-end resequences of the accessions, and the SAMTOOLS software for filtering out the unmapped reads (Li *et al.*, 2009; Li & Durbin, 2010). Duplicated reads were removed by the PICARD package (<http://picard.sourceforge.net/>). The phylogeny was then constructed based on whole-genome single nucleotide polymorphisms (SNPs) using the SNPHYLO software (Paterson *et al.*, 2014) as described by Liang *et al.* (2019). Phylogenetic trees were visualized and coloured using the iTOL browser (<http://itol.embl.de/>).

Plant material

Representative members of sister clades contrasting with respect to their stilbene chemotype of *V. vinifera* ssp. *sylvestris* originating from the last viable population in Germany at Ketsch peninsula, which are available as replicates in the Botanical Garden of KIT, were selected (Duan *et al.*, 2015). The following accessions of *V. sylvestris* representing two different stilbene chemotypes were included in the study: Ke13, Ke28b, Ke30, Ke33 and Ke94 belonged to the PC, while the RVC was represented by Ke15, Ke28c and Ke95. The *vinifera* cultivar Chardonnay, known to be susceptible to GTDs (Guan *et al.*, 2016), and being PC member, was added as a susceptibility reference. For each genotype, wood cuttings were collected from canes, 1 year of age. From 15 March 2018, wood-cuttings (three buds) were cultivated in the glasshouse as potted plants equidistantly (nine plants m⁻²).

Fungal material and inoculation

On 1 June at daytime temperature 26–32°C, plants of each genotype were subdivided into three experimental sets: unwounded individuals, wounded individuals but not inoculated (mock treatment), and wounded individuals were subjected to the full inoculation treatment with *Neofusicoccum parvum* strain Bt-67. The fungal strain was isolated by the Instituto Superior de Agronomia, Universidade de Lisboa, Portugal (Stempien *et al.*, 2017), and kindly provided by the Laboratoire Vigne Biotechnologies et Environnement EA-3991 Université de Haute-Alsace, Colmar, France. For both mock treatment and inoculation, a small hole (3 mm in diameter until reaching the pith area of wood) was drilled into the centre of the pre-annual internode from which the new shoot had emerged (Fig. 1, position B).

To circumvent changes in strain properties due to laboratory cultivation, we used as inoculum mycelia that had been stored in 30% glycerol at –80°C. After thawing, the hyphae were cultivated for 10 d at 27°C on potato dextrose agar (PDA; Sigma-Aldrich), then collected from the agar surface and placed into the hole. The inoculation site was then tightly wrapped with Parafilm. In the mock treatment, after drilling the wood, the wound was directly sterilized with 80% ethanol and then wrapped with Parafilm.

Changes in wood anatomy following inoculation

Wood samples were collected from the infection site 60 d post-infection (dpi) and fixed for 2 d in fixative (4% w/v paraformaldehyde) before washing three times with PIPES buffer (Arend *et al.*, 2002). Afterwards, the samples were dehydrated (Gerlach, 1977) and subsequently embedded in paraffin wax (Paraplast; Carl Roth GmbH, Karlsruhe, Germany). Cross-sections of 20 µm thickness were cut by a microtome (Jung, Heidelberg, Germany) and grouped into different sets stained with different dyes: the first set was stained for lignin for 5 min with 1% (w/v) phloroglucinol (Sigma Aldrich) in 18% HCl; the second set was stained for pectic polysaccharides for 5 min with 0.05% (w/v) Ruthenium Red (Carl Roth); and the third set was stained for 1 min with 0.1% Toluidine Blue (Sigma Aldrich) yielding dark blue for lignin, and a purple for pectic polysaccharides. Images were recorded by digital light microscopy (Zeiss AxioScope and Axio-Cam).

Detection of hyphae through cryo-scanning electron microscopy

Samples were collected and transferred to the Nano imaging Lab, Basel University, to be analysed by cryo-scanning electron microscopy (cryo-SEM; Philips XL30 ESEM) following specimen processing with a Cryo Preparation Unit Gatan Alto 2500. Wood cross-sections of 1 mm thickness were fixed with Tissue-Tek O.C.T glue (Sakura Finetek, Torrance, CA, USA) on a cryo-transfer holder, directly frozen in nitrogen slush and introduced into the cryo unit for observation.

Quantification of wood necrosis, hyphal coverage and xylem vessel cross-section area

To compare fungal responses of the different grapevine accessions, quantitative image analysis was employed, using the IMAGEJ freeware (<https://imagej.nih.gov/ij/>). The length of necrotic spread in a median section of the infected internode was measured as reported by Guan *et al.* (2016) with a slight modification: as readout, necrosis was not represented as affected area relative to the infected internode, because the length of the internode was greatly variable among the genotypes. Instead, the necrotic area was related to the individual internodes, by determining a necrosis score N as

$$N = (N_{\text{inf}} - N_{\text{mock}}) / (N_{\text{total}})$$

where N_{inf} is necrotic area (cm²) in internodes infected by *N. parvum*, N_{mock} is necrotic area (cm²) in internodes subjected to mock inoculation, and N_{total} is total area of the median section of the respective internode.

Hyphal coverage was evaluated for each infected xylem vessel picked up in the cryo-SEM images, through the entire depth of the specimen (1 mm depth) using IMAGEJ.

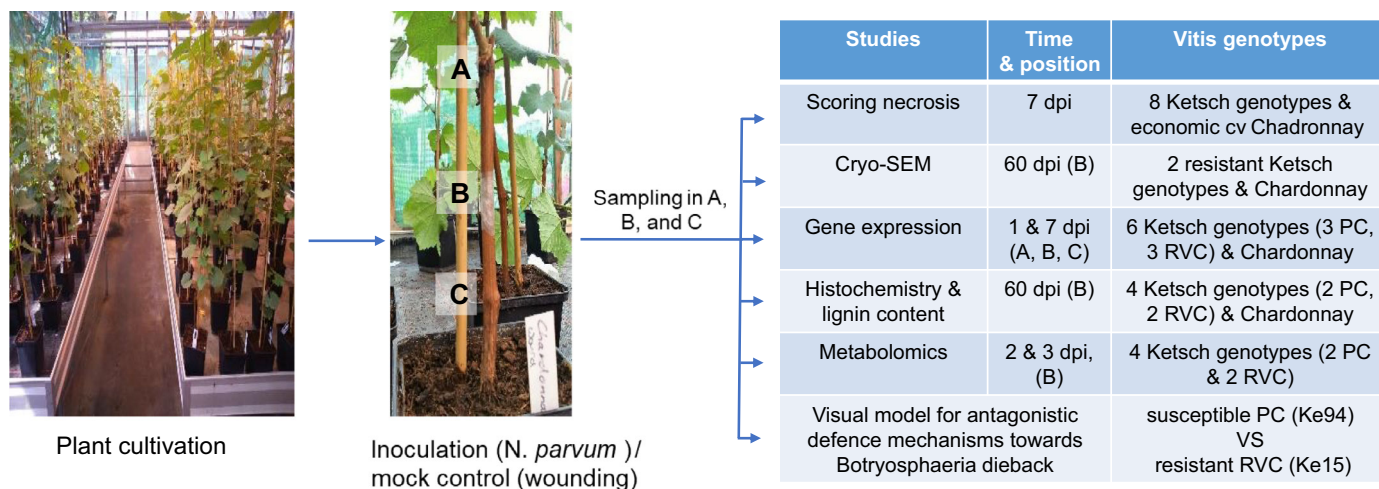


Fig. 1 Experimental design detailing the sample position, and time points (in days post-infection, dpi) for the analysis of gene expression by quantitative real-time PCR, metabolites, scoring necrosis and the different microscopical investigations.

RNA extraction and quantitative real-time PCR

Steady-state transcript levels for defence genes were measured at two time-points, 1 and 7 dpi, as shown in Fig. 1. Total RNA was extracted using the Spectrum Plant Total RNA Kits (Sigma Aldrich) and repurified by using sodium-acetate and ethanol (Walker & Lorsch, 2013). Afterwards, cDNA synthesis and quantitative real-time PCR were conducted as described by Svyatyna *et al.* (2014). *Ubiquitin (VvUBQ)* was chosen as an internal standard. The final result was expressed as \log_2 fold change, derived from the $2^{-\Delta\Delta C_t}$ method (Livak & Schmittgen, 2001), using the control value at day 1 for accession Ke13 as a reference. Primer details are provided in Supporting Information Table S1.

Lignin measurement

Lignin content was quantified in the centre of infected internodes spectrophotometrically after 60 dpi using an acetyl bromide soluble lignin assay (Barnes & Anderson, 2017).

Stilbenes analysis

Wood samples were collected and lyophilized. After grinding the samples using a bead mill (TissueLyser II, Qiagen), metabolites were extracted with 100% methanol ($50 \mu\text{l mg}^{-1}$ wood powder) and analysed using the LC-MS platform at INRAE Grand-Est Colmar (France) as described previously (Duan *et al.*, 2015), with some modifications (Methods S1).

Results

Selection of genotypes based on genome-wide SNP phylogeny

A genome-wide phylogeny constructed from SNPs from 89 *Vitis* genomes, representing European *V. vinifera* varieties, Asian species and American species, in addition to a collection of

European wild grapes (*Vitis vinifera* spp. *sylvestris* (Fig. 2), showed four main clusters. All *V. sylvestris* accessions, from the last viable population in Germany at Ketsch, fell into cluster (I). Asian wild grapes constituted cluster (III), and cluster (IV) comprised American wild grapes. Within cluster (I), several clades could be discerned; the RVC was located in one of the clades, while the PC was spread over several clades.

Susceptibility to *N. parvum* differs between stilbene chemotypes

To assess whether the response to infection with *N. parvum* depends on genotype, we selected RVC genotypes which were genetically close to PC genotypes in a phylogeny designed based on nine SSR markers (Duan *et al.*, 2015). The chosen RVC genotypes Ke15, Ke95 and Ke28c (for which no genome was available) were clustered in pairs with the chosen PC genotypes: Ke13, Ke94 and Ke28b (for which no genome was available) respectively. Further PC individuals were also tested, such as Ke30, Ke33 and Chardonnay. Bark was peeled from the infected and mock-treated canes to examine and quantify the spread of necrosis as a measure of susceptibility at 7 dpi (Fig. 3). The susceptibility was variable, whereby the lowest degree of necrosis was seen in the three representatives of the RVC, while all members of the PC, with the exception of Ke30, were significantly more affected by pathogen-induced necrosis. Thus, RVC is a good predictor for a significantly reduced susceptibility to *N. parvum*, while PC largely correlates with elevated susceptibility.

Wood colonization of *N. parvum* is significantly impaired in hosts of the RVC

To gain insight into the reasons behind the reduced necrosis observed upon infection of genotypes belonging to the RVC, wood colonization was compared by cryo-SEM between *V. vinifera* cv Chardonnay (as representative of the PC), and Ke15 and Ke95, as representatives of the RVC, 2 months after either

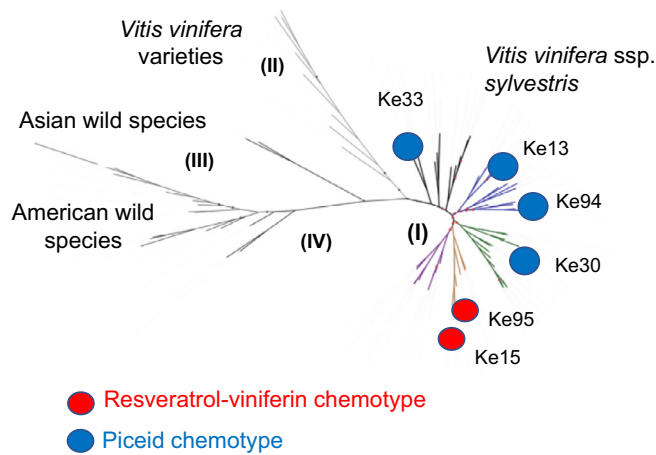
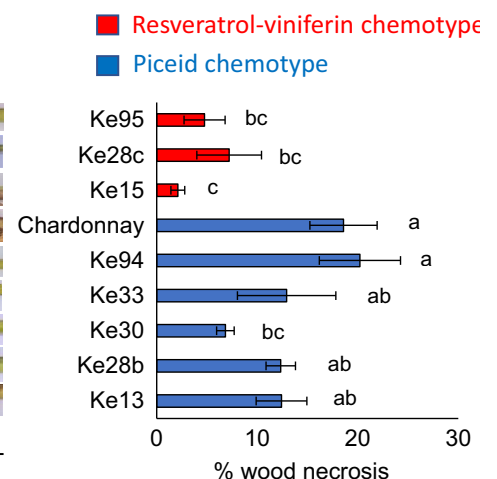
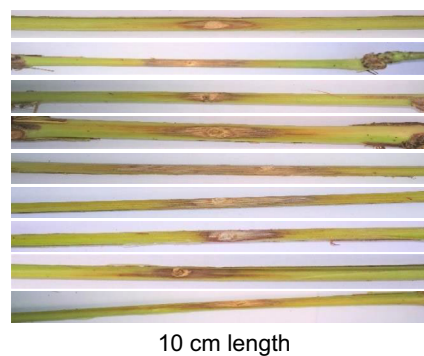


Fig. 2 Position of the genotypes investigated in this study in a phylogenetic tree constructed from genome-wide SNPs for 89 accessions of cultivated *Vitis vinifera* and wild species from Europe, Asia and America. Cluster (I) represents the wild spp. *sylvestris* genotypes from Ketsch, Germany, separated into different clades labelled by colours. Cluster (II) comprises *Vitis vinifera* varieties, Cluster (III) Asian wild *Vitis* species, and Cluster (IV) American wild *Vitis* species. Red circles indicate the resveratrol-viniferin chemotype, while blue circles indicate the piceid chemotype. No genomes were available for Ke28b and Ke28c during the study.

mock treatment or infection (Fig. 4). There was no indication of any fungal growth in sections from mock-treated plants, confirming that the wood was free from endogenous infection (Fig. 4a1–3). In infected plants, irrespective of the genotype, the hyphae were found in xylem vessels, and quite far from phloem, and pith parenchymatic regions. The mycelia were clearly more abundant in the xylem vessels from cv Chardonnay as compared to those of Ke15 and Ke95 (Fig. 4b1–3, c3). This was confirmed by quantification of hyphal coverage across the xylem vessel cross-section area (Fig. 4d). Here, Ke15 showed values that were around 20% of those seen in cv Chardonnay. For the more susceptible Ke95, coverage was around 40% of those found in cv Chardonnay. The same genotypes, Ke15 and Ke95, had also displayed the lowest degree of wood necrosis after 7 dpi (Fig. 3), with Ke15 being superior in resistance over Ke95, exactly

Fig. 3 Susceptibility of *sylvestris* genotypes from different stilbene chemotypes, and the *vinifera* variety Chardonnay to *Neofusicoccum parvum* strain Bt-67. Susceptibility was quantified as the proportion of necrotic cross-section area corrected for the area of wound-damaged area over the cross-section of a 10 cm internode segment. Representative images of each infected genotype are shown in the left-hand panel, and corresponding means and standard errors from three individuals per genotype are given in the right-hand panel. Different letters after the bars indicate statistical differences among infected genotypes at $P < 0.05$.



mirroring the values obtained for hyphal coverage 2 months later. This demonstrates that wood necrosis on the outer surface, beneath the phloem measured after 7 dpi, can be used as a reliable indicator of susceptibility of a genotype.

Resistance to fungal spread correlates with accumulation of resveratrol and viniferins

To test whether the variable necrosis scores among Ketsch accessions is related to a distinctive phytoalexin profile, we sampled three or four biological replicates at 2 and 3 dpi in the centre of inoculated internodes for a set of four *sylvestris* genotypes of varying susceptibility (Ke13 and Ke94 as representatives of the PC; Ke15 and Ke95 as representatives of the RVC). Fourteen stilbene derivatives and their precursors phenylalanine, tyrosine and *p*-coumaric acid were measured and normalized to the value found in nonwounded plants of Ke13 at day 2 (Fig. 5a,b). For all tested genotypes, wound treatment alone induced *p*-coumaric acid, and *trans*- and *cis*-resveratrol, as well as their derivatives piceatannol, δ -viniferin, and viniferin trimers 1 and 2 (Figs 5a, S1). In the infected plants of all genotypes, piceatannol and *cis*- ϵ -viniferin accumulated beyond the levels seen for wounding alone. Infection accelerated the accumulation of *trans*- and *cis*-resveratrol, in addition to α -viniferin. This was prominent at 2 dpi, while these compounds accumulated more slowly for wounding alone (Fig. S1).

In the background of this qualitative general pattern, there were clear differences in amplitude and time course of these metabolite profiles. Generally, for the genotypes representing the RVC, stilbenes accumulated more rapidly and intensively as compared to the PC genotypes, which was true for both wounding alone and infection (Fig. 5). In particular, both Ke15 and Ke95 accumulated more *trans*- and *cis*-resveratrol than any of the PCs at 2 dpi for wounding alone. Regarding infection, Ke15 exhibited the highest levels of the stilbene precursors tyrosine and *p*-coumaric acid, and nonglycosylated stilbene monomers as early as 2 dpi. For instance, *trans*-resveratrol was induced 41-fold and *cis*-resveratrol even 82-fold in Ke15, while the two PCs produced 27- to 28-fold more *trans*-resveratrol, and only about two- to three-fold more *cis*-resveratrol. For resveratrol oligomers, stilbene

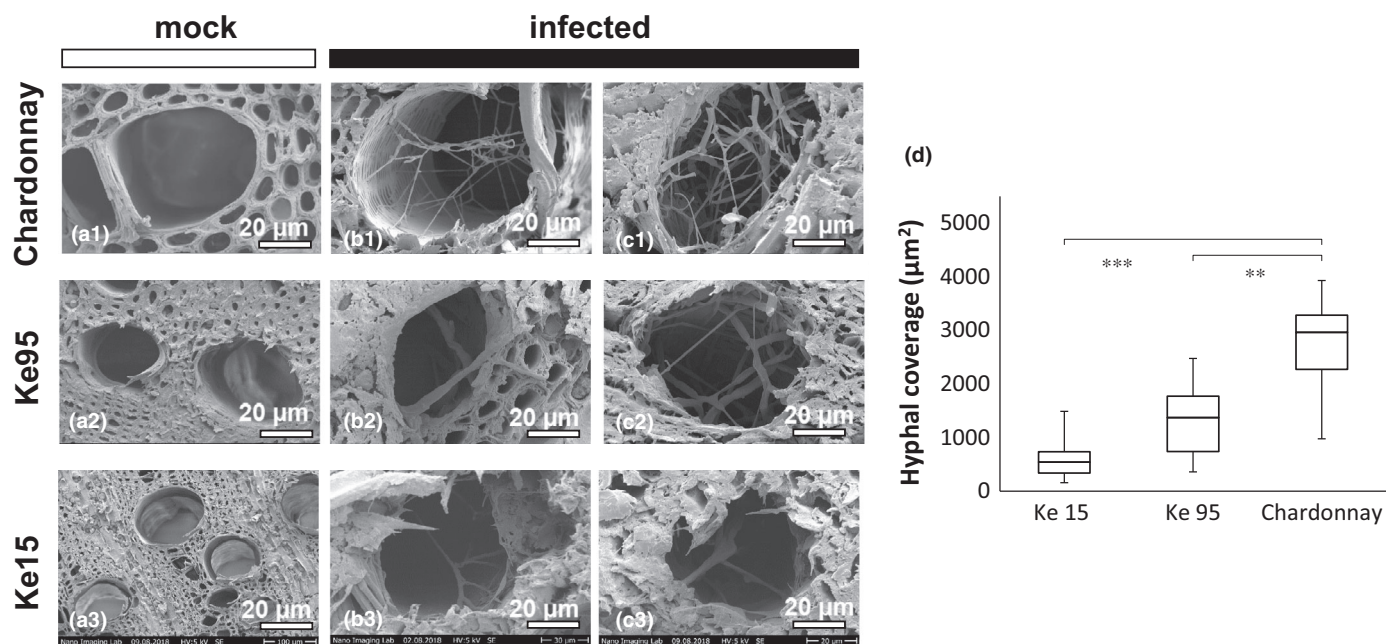


Fig. 4 Colonization of xylem vessels in the variety Chardonnay compared to the *Vitis sylvestris* genotypes Ke15 and Ke95 (belonging to the resveratrol–viniferin chemotype). (a–c) Representative cryo-SEM images from mock-treated (a) and infected (b, c) internodes, 2 months after the respective treatment. Infection was conducted with *Neofusicoccum parvum* strain Bt-67. (d) Quantification of hyphal growth. Whisker and box plots showing median and interquartile range of hyphae growth area per infected xylem vessel (1 mm depth) of three biological replicates. Asterisks represent significant differences among means of hyphae growth area through the infected xylem vessels. **, $P < 0.01$; ***, $P < 0.001$.

dimers and trimers, significant accumulation of *trans-ε*-viniferin, specific for infection, was seen only in Ke15 at 2 dpi, while *cis*- and *trans-δ*-viniferins increased at 3 dpi in this genotype. Likewise, infected Ke15 ranked first in the induction of the stilbene trimers (α -viniferin, viniferin trimers 1 and 2). In particular, viniferin trimer 2 increased from six- to 13- fold at 3 dpi in Ke15, while it remained at about five-fold for the infected PCs at the same time point. Also for Ke95, infection led to higher levels of both *trans*-resveratrol (41-fold) and *cis*-resveratrol (31-fold) at 2 dpi, followed later by increased levels of viniferins trimers 1 and 2, as compared to the PCs (Figs 5a,b, S1). This increase in stilbene aglycons of the two genotypes, belonging to the RVC, was accompanied by a significant reduction in piceid, as expected from the preferential allocation of resveratrol to viniferin derivatives.

To look for further evidence of correlation between the RVC and resistance against Botryosphaeriaceae-related dieback, genomic DNA was extracted via the CTAB method (Cota-Sánchez *et al.*, 2006) from the infection site of an RVC representative (Ke15), and the most susceptible PC (Ke94) to estimate the abundance of *N. parvum* DNA (Method S1; Fig. S2). After 60 dpi, the *N. parvum* molecular marker bp-1-42 (Baskarathavan, 2011) showed that the fungal DNA was about three times more abundant in Ke94 as compared to Ke15.

Susceptible genotypes respond to infection by a higher deposition of lignin

The lignin pathway competes with stilbene synthesis for the same precursors deriving from phenylalanine. To assess the

consequences of infection on the partitioning between these competing pathways, the expression of two key genes for lignin biosynthesis, *caffeic acid O-methyltransferase* (*VvCAOMT*) and *cinnamyl alcohol dehydrogenase* (*VvCAD*) were tested at 1 and 7 dpi. Wood samples were collected from cv Chardonnay and the *sylvestris* genotypes used in the metabolite analysis, that is Ke13, Ke15, Ke94 and Ke95 (Fig. 6a,b). With the exception of Ke94, there were no significant fluctuations in steady-state levels of *VvCAOMT*. In Ke94, this transcript was strongly upregulated in infected plants compared to mock-treated plants or any other infected genotypes at 1 dpi, and was still elevated until 7 dpi. However, at this time point, *VvCAOMT* transcripts in wounded plants had increased to a level exceeding that of infected plants. For *VvCAD*, the genotypes tested at 1 dpi showed no significant induction in response to infection or to the mock-treatment. However, after 7 dpi, *VvCAD* was upregulated in wounded and infected Ke94. This was not seen in the other genotypes under different treatments, except wounded Ke95.

Variations in lignin accumulation over 60 dpi were quantified spectrophotometrically (Fig. 6b), and qualitatively by histochemical staining (Fig. 6c,d) in the tested genotypes for *VvCAOMT* and *VvCAD* expression analysis. Compared to mock-treated plants, the staining for both lignin assays, Phloroglucinol-HCl, or Toluidine Blue, increased in infected plants (Fig. S3). Likewise, Ruthenium Red, staining for pectins, exhibited an increased signal upon infection (Fig. S3).

By contrast, there were variations in colour intensity between the stained reaction zones (RZs) among infected genotypes (Fig. 6c,d). In particular, the RZ of infected Ke94 was stained more intensively with both lignin assays compared to any of the other

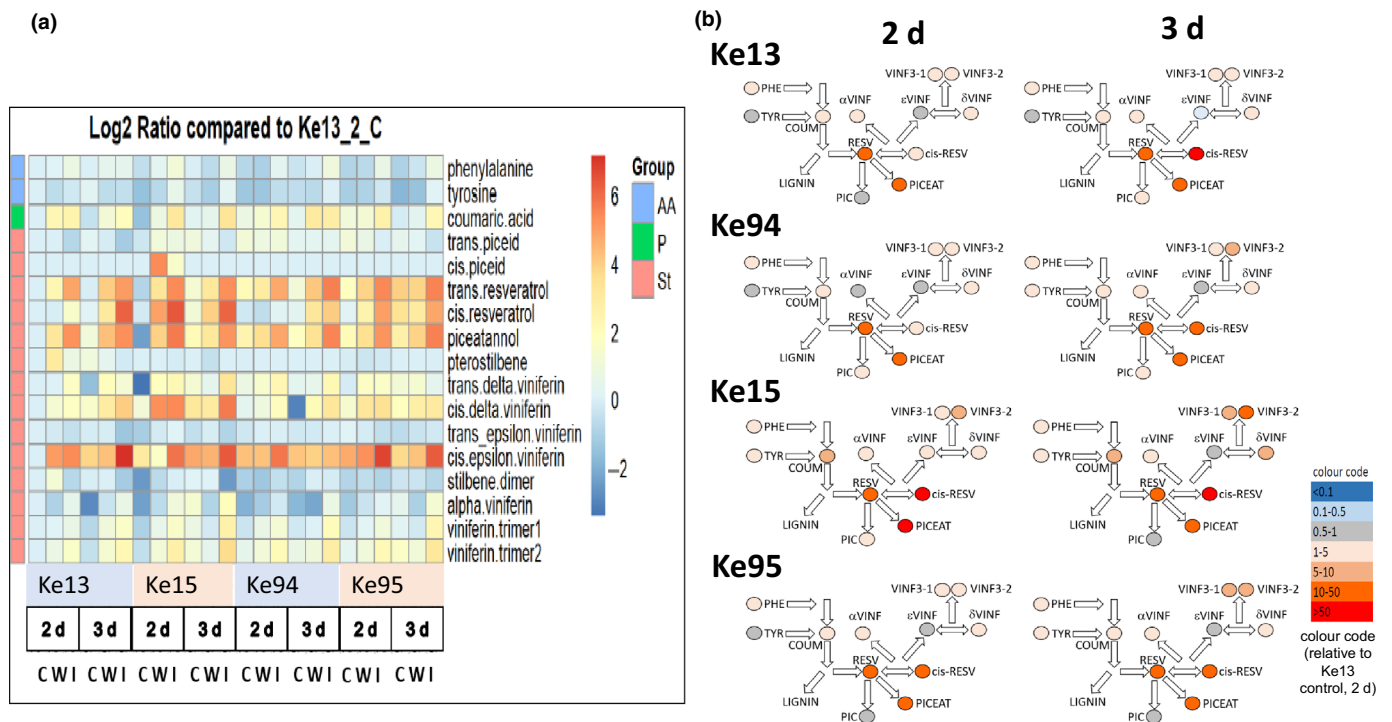


Fig. 5 Heat map of metabolite abundance in response to infection with *Neofusicoccum parvum* strain Bt-67 at the infection site in four *sylvestris* accessions measured 2 and 3 d post-infection (dpi). (a) Log₂ ratios of mean metabolite abundance in untreated controls (C), wounded, noninfected (W) and infected (I) plants as compared to the control Ke13 at day 2. Metabolites are grouped into amino acids (AA), phenylalanine derivatives (P) and stilbenes (St). (b) Different redistribution of phenylpropanoid metabolism in response to infection at 2 and 3 dpi after normalization to the control Ke13 at day 2. Colour code represents fold changes. Data represent mean values of three or four biological replicates for each genotype and time point. Statistical analysis was performed using Tukey's test, with $P \leq 0.05$.

genotypes. Also, Ke13 and cv Chardonnay showed intensified lignin staining around the infected xylem vessels. By contrast, the two tested accessions of the RVC produced a much lighter staining. In particular, infected Ke15 did not show a prominent increase in lignin deposition through histological staining. To confirm this quantitatively, lignin was extracted from the central internode around the wound and quantified spectrophotometrically (Fig. 6b). Here, the three tested piceid genotypes showed a significant increase of lignin in infected over mock-treated plants, with the highest levels found in Ke94. This increase was not seen in the accessions of the RVC, and for Ke15, lignin accumulated even less upon infection as compared to wounding alone. Thus, the histochemical pattern observed (Fig. 6c,d) was confirmed by the quantification of extracted lignin (Fig. 7b).

Resistance to fungal spread correlates with inducibility of stilbene synthase transcripts

To gain insight into a potential reason behind differences in metabolites between the RVC and PC, whether it is driven by gene expression or enzyme activities, we measured steady-state transcript levels of selected phytoalexin biosynthesis genes. These included phenylalanine ammonia-lyase, *VvPAL*, representative members of the different stilbene synthase clades *VvSTS6*, *VvSTS16*, *VvSTS27*, *VvSTS47*, (Parage *et al.*, 2012; Vannozzi *et al.*, 2012), and *VvJAZ1*, reflecting the status of basal defence (Fig. 7).

Steady-state levels of the transcripts at the infection site (Fig. 7b) showed a consistent upregulation at 1 dpi in response to infection that clearly exceeded the upregulation seen for wounding alone. However, the amplitude of this induction was not only dependent on the respective transcript but also on the genotype. The highest abundance was observed for Ke94, irrespective of transcript. However, ground levels for *VvJAZ1* and *VvSTS47* were already strongly elevated in Ke94 (Fig. 7). Omitting Ke94, the induction was consistently more pronounced in the RVC genotypes Ke28c and Ke95, as compared to the PC genotypes Ke13, Ke28b and cv Chardonnay (Fig. 7b). The RVC, Ke15, followed a different pattern: in response to infection, the steady-state levels were lower than in the other two tested RVCs. However, the resting levels under control conditions were much lower in Ke15 than in the other genotypes (Fig. 7b). To gain insight into a potential link of the stilbene synthase transcripts with jasmonate signalling, the response of *VvSTS6*, *VvSTS16* and *VvSTS47* to methyl jasmonate was assessed in a *V. rupestris* cell culture (Fig. S4) as an approximation to the situation in the wood itself, where this experiment would be difficult to conduct with the necessary precision. Furthermore, this gene induction due to infection did not persist over time and had generally declined at 7 dpi (Fig. 7b).

In a different approach, we probed for a potential systemic spread of the defence response at 1 dpi (Fig. 7a,c). In the most heavily colonized line, Ke94, all tested genes of the

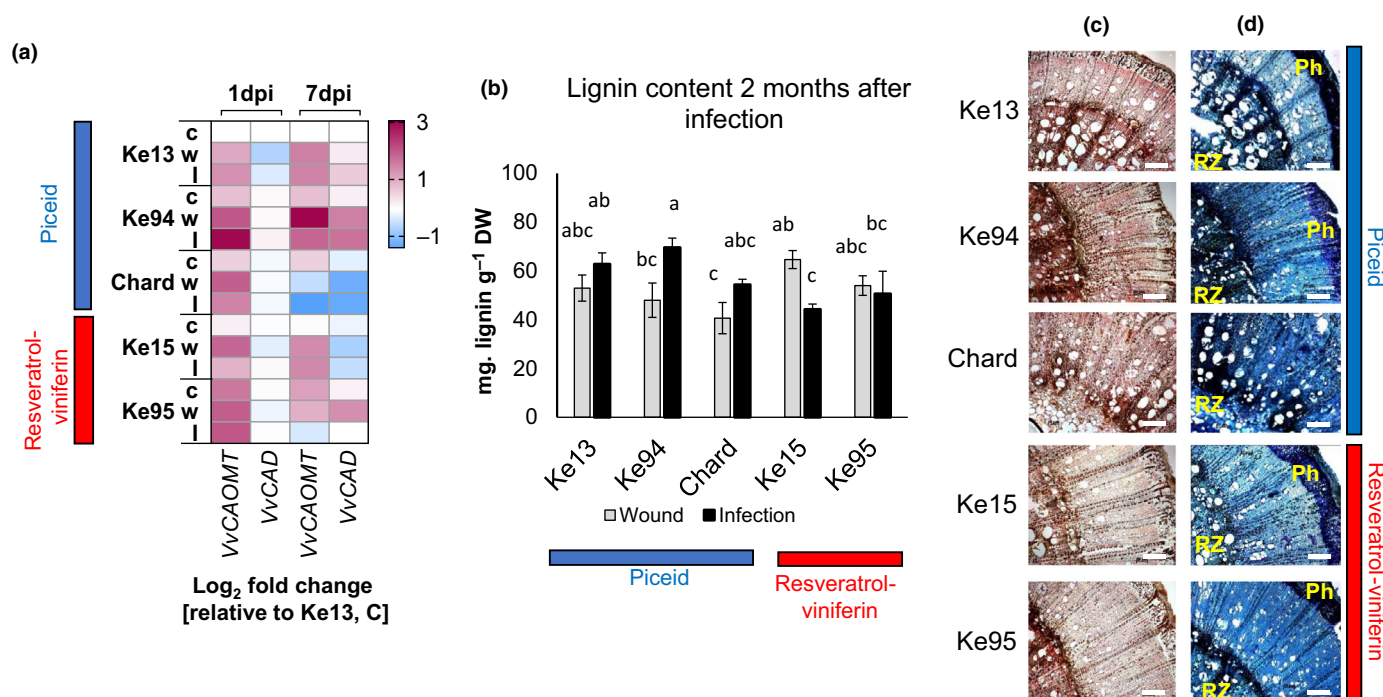


Fig. 6 Genotypic differences in lignin metabolism in response to *Neofusicoccum parvum* strain Bt-67. (a) Heat map showing the \log_2 fold changes in steady-state transcript levels of the two lignin-biosynthesis genes *VvCAOMT* and *VvCAD*, at infected (I), and mock treatment (wounding only, W) over the untreated controls (C) and normalized to the levels in control Ke13 plants at two time points; 1 d postinfection (dpi) and 1 wk (7 dpi) post infection. (b) Lignin content at 2 months after infection at the infection site at wounded and infected canes. Different letters specify the statistical significances among the genotypes in lignin content using Duncan's test with $P < 0.05$ (*). Error bars indicate the standard error and three biological replicates were counted for each assay related to biosynthesis and the content of lignin. (c, d) Histochemical staining of cross-sections at the infection site 2 months after infection, with Phloroglucinol-HCl staining lignin in light red or rose (c), and Toluidine Blue staining lignin in blue, and pectic polysaccharides in purple (d). RZ, reaction zone of the plant–fungal interaction; Ph, phloem. Bars, 100 μm .

phenylpropanoid pathway (*VvPAL*, *VvSTS27* and *VvSTS47*), and *VvJAZ1*, were significantly upregulated, both from 4 cm to the base or to the tip of the infection site. This was not seen in the other genotypes, except the tip of PC Ke13. There was also a clear directionality, because *VvJAZ1* was more induced apically as compared to the base in all plants. Following the persistence of this systemic response in Ke94 at 7 dpi, we noted that the induction of *VvPAL*, *VvSTS27* and *VvSTS47* had generally eased off, but significantly less in the distal sites. Moreover, the transcript levels of *VvJAZ1* were higher in the apical site, although the difference between infection and wounding control was, with the exception of Ke13, not significant.

In summary, activation of phytoalexin genes remained mostly confined to the infection site. Only in Ke94, where colonization was progressing most rapidly, did the distant position (in particular the one apical site) show induction of these genes. This systemic response therefore cannot be used as an indicator of resistance, but rather for susceptibility and might represent a local response to the rapidly spreading fungus.

Bordered pits act as gateways for fungal spread

Cryo-SEM imaging of infected wood from the susceptible variety cv Chardonnay appeared to exhibit steps in the hyphal colonization process (Fig. 8). For instance, bordered pits perforating the

later walls of xylem vessels (Fig. 8a) appear to provide spatial cues for the orientation of hyphal growth during early colonization (Fig. 8b). After complete attachment to the wall, new hyphae reach out towards the bordered pits of the opposing wall, creating a mycelium with a geometric growth pattern (Fig. 8c). The hyphae then penetrate through the bordered pits from infected vessels in a radial direction into the para-tracheal parenchymatic cells, thereby increasing horizontal fungal spread (Fig. 8d,e). During later stages, the mycelium not only completely blocks the xylem vessels (Fig. 8f), but also uses cracks in the *Vitis* wood for further spread (Fig. 8g).

Because the high susceptibility of certain varieties had been explained by a higher vessel diameter (Pouzoulet *et al.*, 2014, 2017), the mean cross-section area from 50 individual xylem vessels obtained from the internode centres was determined for different genotypes (Fig. 8h) to look for a potential correlation with necrosis area. Vessel cross-section areas were significantly smaller in the *sylvestris* accessions compared to cv Chardonnay. However, the resistant genotypes Ke15 and Ke95 did not display narrower vessels as compared to the susceptible genotypes Ke13 and Ke94. By contrast, the smallest vessel cross-section area was found for the susceptible Ke94. Concerning stem cross-section area and relative coverage of pith area, there was no observed architecture pattern that could be used as a cue for resistance or to differentiate between the PC and the RVC (Fig. S5). A correlation

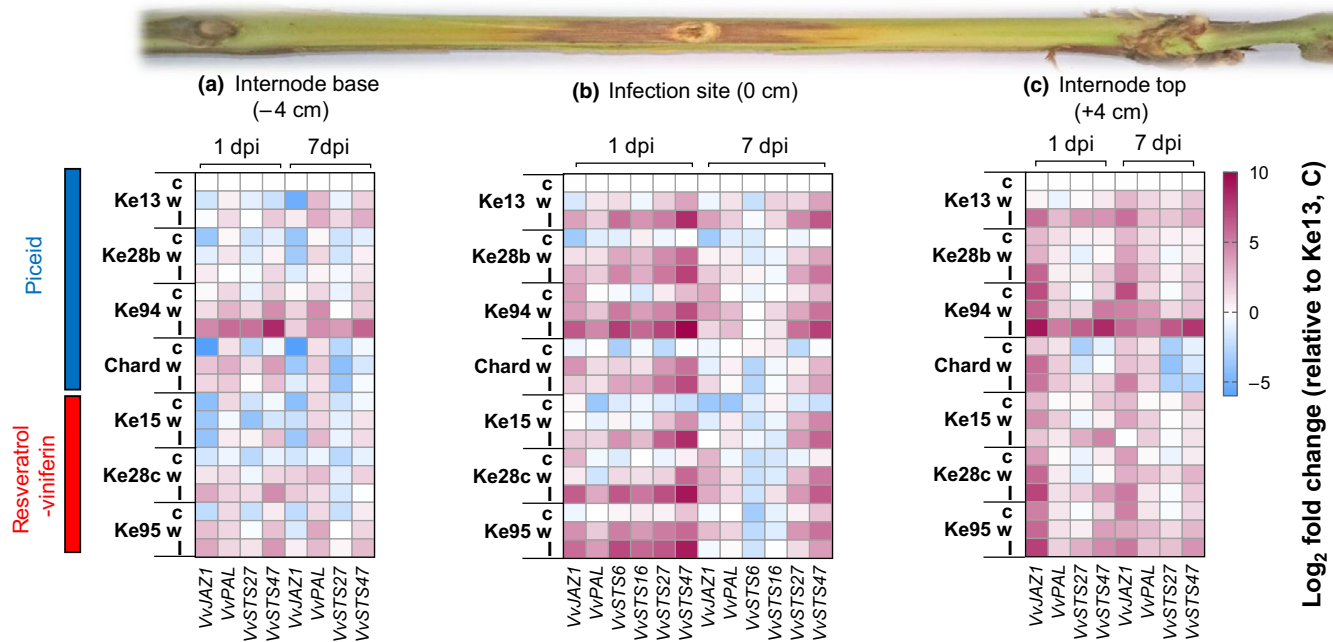


Fig. 7 Heat maps showing \log_2 fold changes in steady-state transcript levels of defence-related genes (*VvJAZ1*, *VvPAL*, *VvSTS6*, *VvSTS27*, *VvSTS47*, *VvSTS16*) in genotypes belonging to the piceid (Ke13, Ke28b, Ke94, cv Chardonnay) and the resveratrol-viniferin (Ke15, Ke28c, Ke95) chemotypes by RT-qPCR after 1 d and 1 wk of infection. For each genotype, transcript levels for control (unwounded), mock (wounded) and infected plants were analysed at three positions: internode base (a), infection site (b) and internode top (c). Colour code represents \log_2 fold changes in transcripts levels normalized first relative to expression levels in control plants of the piceid chemotype (Ke13). Data represent mean values from three biological replicates per each genotype and time point. dpi, days postinfection.

between genotypic differences of wood anatomy and infection could not be established.

Discussion

We screened *V. vinifera* ssp. *sylvestris*, the ancestral species of cultivated grapevine (*V. vinifera* ssp. *vinifera*) for resistance against GTDs. We detected a correlation between velocity and amplitude in the accumulation of resveratrol and viniferins and resistance. In the following, we discuss the potential and limitations of our experimental system, the role of wood anatomy for susceptibility, and a working model, where genetic factors partitioning phenylpropanoid metabolism between the stilbene and the lignin branch contribute to resistance.

A minimal experimental system to study resistance against *N. parvum* in vivo

Long-term aspects, such as the characteristic leaf discoloration or apoplectic breakdown that are usually observed after years of colonization, when the fungus emerges from its latent phase to kill the host in a few days (Bertsch *et al.*, 2013) cannot be investigated. An *in planta* inoculation assay (Fig. 1) applying combined chemo-analytical and morpho-analytical approaches allowed us to analyse a specific strain related to Botryosphaeriaceae-related dieback, *Neofusicoccum parvum* Bt-67, to address *in vivo* genetic, molecular and cellular factors contributing to resistance during the early phase of colonization. In this study, the extent of wood

necrosis was used as an operational definition for resistance to Botryosphaeriaceae-related dieback in the respective genotype. The correlation of hyphal growth in xylem vessels after 60 dpi (Fig. 4d) with the wood necrosis area measured after 1 week (Fig. 3) in infected Ke15 and Ke95 vs infected cv Chardonnay supports the predictive value of our assay to judge the resistance against fungal invasion. The results from our assay show that there is a significant difference between the genotypes, although they originate from one population. Our genome-wide SNP analysis revealed that this population formed a separate clade within the genus *Vitis*, distinct from *V. vinifera* ssp. *vinifera*, and distinct from wild species from America or East Asia, consistent with the phylogenetic data from a more extensive set of 472 accessions (Liang *et al.*, 2019). Interestingly, the last viable population of *V. vinifera* ssp. *sylvestris* in Germany still harboured considerable genetic diversity and was compared to other European populations of *sylvestris* and autochthonous *vinifera*. The reason for this high diversity in a relict population might be linked to the post-glacial migration of this species, typically occurring in alluvial forests along major rivers. A major selective pressure for alluvial species is hypoxia. Boosting stilbene aglycons for oxidative balance during flooding would, as a side effect, also generate a higher level of basal immunity in RVCs, even for pathogens, where there was no co-evolutionary history, such as downy mildew, powdery mildew and black rot, which entered Europe only in the late 19th century and, therefore, can be ruled out as selective drivers of a gene-for-gene type resistance (Schröder *et al.*, 2015). In addition, GTDs, with their pronounced

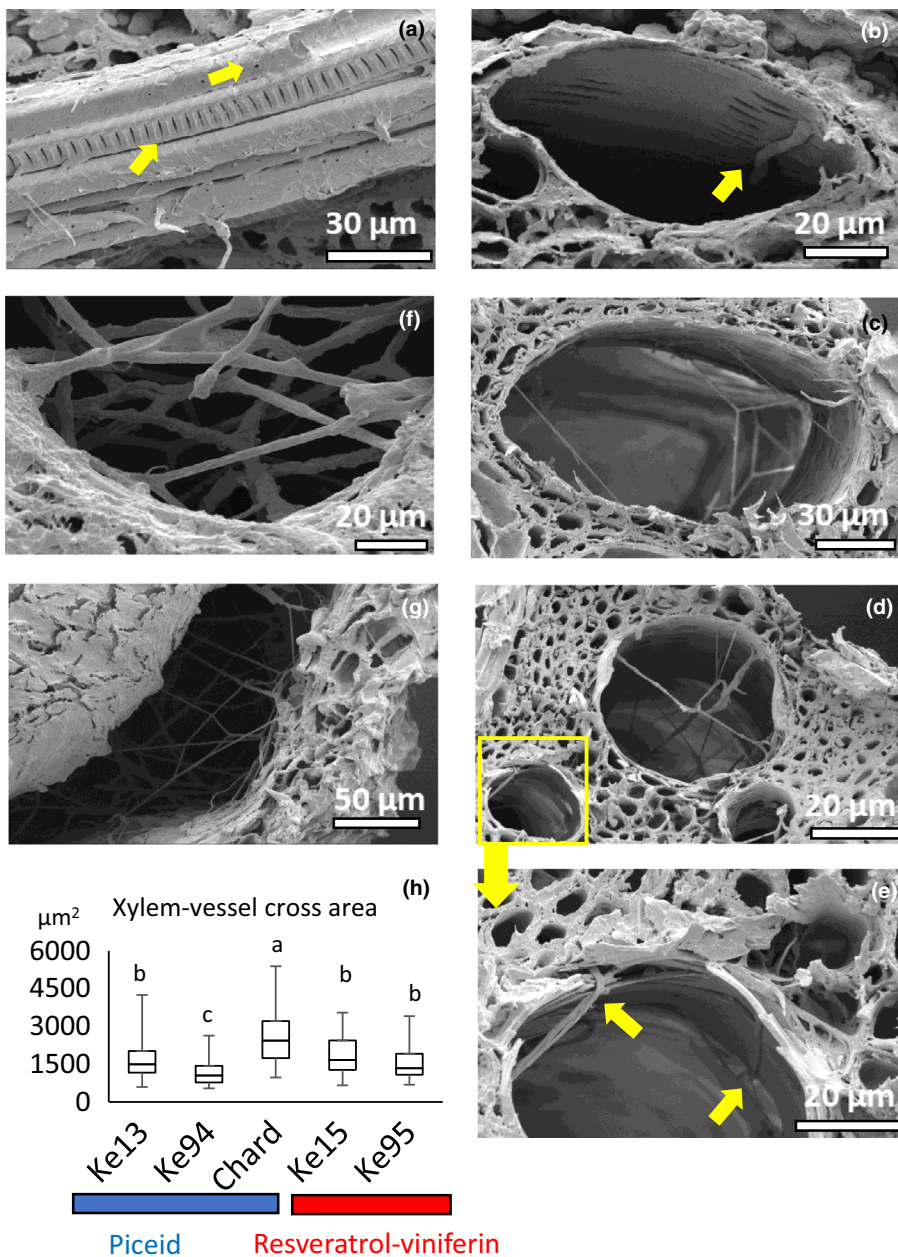


Fig. 8 Cryo-SEM images showing cellular details of colonization of *Neofusicoccum parvum* strain Bt-67 in infected cv Chardonnay xylem vessels. (a) Longitudinal section of xylem vessel displaying bordered pits. (b) A fungal hypha probing the xylem bordered pits during an initial stage of growth. (c–e) *N. parvum* hyphae growing in a geometrical pattern utilizing the bordered pits for horizontal growth or colonization of neighbouring vessels (yellow arrows). (f, g) Fungal mycelia blocking the xylem vessels and spreading through wound cracks during late infection. (h) Whisker and box plots displaying median and interquartile range of xylem vessel cross-section areas of *Vitis vinifera* cv Chardonnay, and four *sylvestris* accessions belonging to different chemotypes (Ke13, Ke94, Ke15, Ke95). Data represent medians from 50 individual vessels from three biological replicates per genotype and statistically differentiated using Duncan's test.

association with drought stress, are highly unlikely as selective factors under conditions found in an alluvial forest. Among the nine tested accessions, the two most resistant genotypes, Ke15 and Ke95, belonged to the RVC, while the other, more susceptible genotypes belonged to the PC (Duan *et al.*, 2015). Thus, our reductionist system not only truly predicts the long-term colonization of xylem vessels, but also reflects chemotype differences derived from metabolic analysis.

Differences in wood architecture do not correlate with resistance

Previous studies have suggested, based on a comparison with three commercial *vinifera* varieties, that xylem vessel diameter is a

predictor for fungal spread of Esca diseases in grapevines (Pouzoulet *et al.*, 2014, 2017). Our study does not show any correlation between xylem vessel geometry and resistance to Botryosphaeriaceae-related dieback (Fig. 8h). While the resistant genotypes Ke15 and Ke95 predicted by this hypothesis to have the smallest vessels failed to show this, Ke94, which ranked as the most susceptible genotype, had the smallest xylem vessels and was similar with respect to fungal necrosis to the susceptible *V. vinifera* cv Chardonnay (Fig. 3), although its vessels had twice the width (Fig. 4). This lack of correlation is not surprising, because the fungal hyphae do not remain confined to the infected xylem vessels, but escape horizontally from the vessel through the bordered pits without need to breach the walls of further vessels (Fig. 8). Because we could not detect a significant correlation

between wood architecture and pathogen spread, we tested whether chemical defence mechanisms (such as phytoalexin accumulation) might play a role.

Resveratrol–viniferin metabolism as resistance factor against *Botryosphaeriaceae* infection

The *sylvestris* genotypes Ke15 and Ke95 performed best in restraining wood necrosis (Fig. 3), and efficiently reduced hyphal coverage in colonized vessels (Fig. 4). Both genotypes belong to the RVC (Duan *et al.*, 2015), and accumulated more of the stilbene aglycons, especially resveratrol and viniferins (Fig. 5). The antimicrobial properties of stilbenes are well established and can act on different levels, such as spore release or germination, or inhibition of fungal pectolyases and hydrolases (Langcake, 1981; Kumar & Nambisan, 2014). A role for stilbenes as resistance factors has been demonstrated for several diseases affecting *Vitis* including downy mildew, powdery mildew and grey mould (Adrian & Jeandet, 2012; Duan *et al.*, 2015; Kelloniemi *et al.*, 2015; Jiao *et al.*, 2016). Hyphal growth rates of *N. parvum* *in vitro* were found to be inhibited by resveratrol or viniferins (Stempien *et al.*, 2017).

Elevated levels of the stilbene aglycon resveratrol are followed by its oligomerization into different viniferin derivatives (Keylor *et al.*, 2015), which can explain the observed patterns (Fig. 6): In the resistant genotypes Ke15 and Ke95 even by 2 dpi, both *cis*- and *trans*-resveratrol were conspicuously elevated over the values seen in the susceptible genotypes Ke13 and Ke94. This was followed, 1 d later, by higher accumulation of the stilbene oligomers δ -viniferin, and viniferin trimers 1 and 2. These stilbene oligomers are therefore correlated with resistance against *N. parvum*. This accumulation is specific, as some stilbene oligomers, such as *cis*- ϵ -viniferin, are found in both susceptible and resistant genotypes. Although *cis*- ϵ -viniferin has been found to accumulate in sites infected by *Plasmopara viticola* (Pezet *et al.*, 2004), this correlation does not prove bioactivity, but might be a side phenomenon produced by the synthesis of other, bioactive, oligomers. In fact, *cis*- ϵ -viniferin was reported as a detoxification product converted from *trans*-resveratrol by laccases secreted by the causative agent of grey mould, *Botrytis cinerea* (Breuil *et al.*, 1999). In addition, the accumulation of ϵ -viniferin during advanced wood decay, such as red wood rot in the context of Esca syndrome, would qualify this stilbene oligomer rather as a by-product, not as a bioactive phytoalexin (Amalfitano *et al.*, 2000).

The susceptible genotypes Ke13 and Ke94 accumulated significantly less viniferins as compared to the resistant lines. However, both Ke13 and Ke94 had accumulated more piceid at 3 dpi (Fig. 5b), followed by significantly higher abundance of lignin 2 months later (Fig. 6b). Interestingly, transcripts levels of all tested defence genes (*VvSTS*, *VvPAL*, *VvJAZ1*) were higher in Ke94 than in any other tested genotype (Fig. 7). Thus, this genotype is definitely responsive to the fungus. However, this induction of transcripts does not culminate in efficient resistance against fungal spread. The reason for this might be that this genotype accumulates piceid, which seems to lack bioactivity against

the pathogen, consistent with results obtained for the pathogen *Plasmopara viticola*, where accumulation of this stilbene glucoside was not able to contain infection (Alonso-Villaverde *et al.*, 2011; Duan *et al.*, 2015). Thus, activation of stilbene synthesis transcripts at an early stage appears to be insufficient to inhibit fungal spread. To be effective, this activation probably needs to be part of a wider process in which resveratrol is channelled towards nonglycosylated viniferins.

Resistance or susceptibility: a matter of channelling phenylpropanoid metabolism?

Our study combining different levels of analysis (physiology, histology, gene expression, metabolites) leads to a working model explaining the observed differences of susceptibility to *N. parvum* by differential channelling of phenylpropanoid metabolism (Fig. 9), providing an example of the contrasting allocation of the phenylpropanoid pathway between a resistant (Ke15) and a susceptible (Ke94) genotype. The higher observed susceptibility in the PC model (Ke94), relative to the RVC model (Ke15), was not only documented by the higher necrosis score after 7 dpi (Fig. 3), but also by the higher abundance of fungal DNA at 60 dpi; that is, at a late time point that is relevant for the situation in the vineyard (Fig. S5). Infection activates defence signalling, conveyed by several parallel pathways; for the sake of simplicity, only jasmonate signalling is shown (Fig. 9, ①, ②) which acts as an upstream signal activating the phenylpropanoid pathway (Tassoni *et al.*, 2005). An implication of this model would be that activation of jasmonate signalling should induce transcripts of phytoalexin synthesis. While this is difficult to be tested in wood, this could be confirmed using *Vitis rupestris* suspension cells as an approximation (Fig. S4).

The specific and rapid activation of *VvSTS27* and *VvSTS47* transcripts (Fig. 9, ③) is followed in Ke15 by accumulation of *p*-coumaric acid and tyrosine, and the vigorous synthesis of *trans*- and *cis*-resveratrol (Fig. 9, ④), followed by strong oligomerization to nonglycosylated resveratrol trimers (α -viniferin, viniferin trimer 1 and viniferin trimer 2, Fig. 9, ⑤). Whether all of these stilbene derivatives that appeared abundantly in infected Ke15 plants (more than in any other genotype) are strong phytoalexins remains to be elucidated. Some of them, such as the stilbene monomer *cis*-resveratrol or the stilbene dimer δ -viniferin might represent transient precursors for the viniferin trimers which accumulate 1 d later. In the susceptible Ke94, the significant accumulation of *STS* transcripts levels does not lead to a corresponding accumulation of resveratrol (delayed by 1 d as compared to Ke15). Furthermore, compared to Ke15, Ke94 allocated more resveratrol to the glycosylated piceid (Fig. 9, ⑥), accompanied by a lower amplitude and a temporal delay in the accumulation of *trans*- and *cis*-resveratrol and viniferin trimers. In addition, Ke94 deposited more lignin around the infected vessels (Fig. 9, ⑦), as revealed by histological staining, transcripts levels of *VvCAOMT* and *VvCAD*, and quantification of extracted lignin (Fig. 6). This excessive deposition of lignin deposition was also seen in all tested accessions belonging to the PC (Ke13, Ke94, cv Chardonnay).

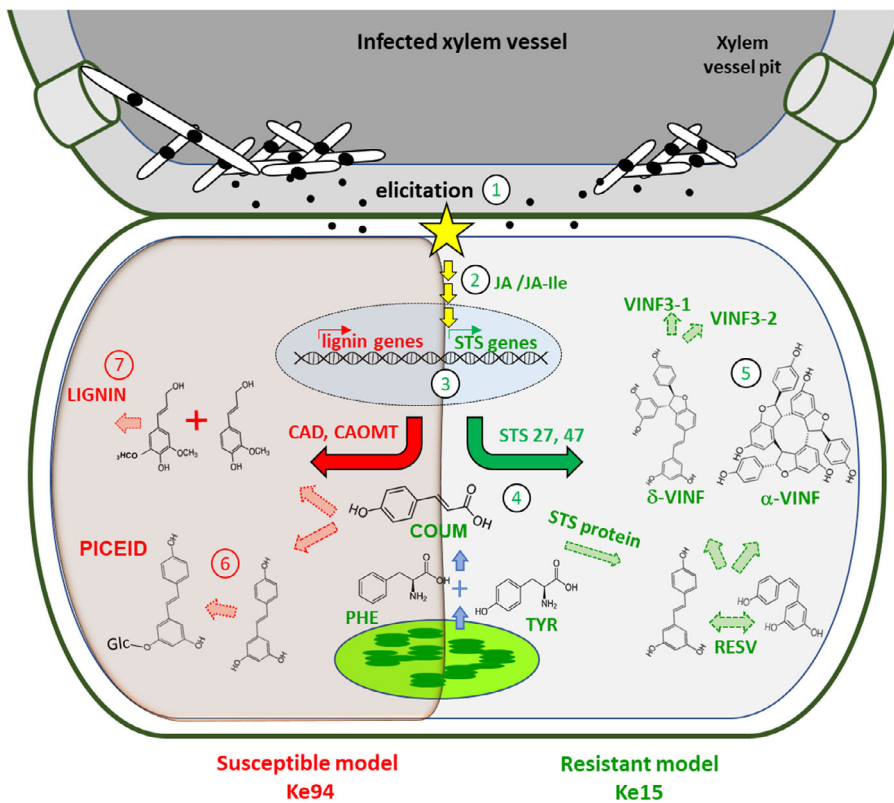


Fig. 9 Visual model representatively illustrating the difference in the response to *Neofusicoccum parvum* in a resistant (Ke15) vs a susceptible genotype (Ke94) through differential allocation of the phenylpropanoid metabolism. For details see the Discussion section.

While our study does not find any evidence that wood architecture is relevant for fungal spread, because the fungal hyphae use bordered pits for vessel-to-vessel colonization, we conclude that fast and robust channelling of the phenylpropanoid pathway towards the stilbene aglycon resveratrol and subsequent oligomerization into viniferins is a core resistance factor. This channelling is under genetic control, because it is found in accessions belonging to the RVC, while accessions belonging to the PC partition the pathway towards glycosylated piceid and even the formation of lignin. While lignin has been proposed as a resistance factor for the leaf pathogen *Plasmopara viticola* (Dai *et al.*, 1995), it does not qualify as such in a wood-decaying fungus, but rather is expected to support further spread. While a strong induction of stilbene synthase transcripts is a prerequisite for phytoalexin accumulation, it is by no means a sufficient condition, as illustrated by the example of Ke94. In this genotype, the accumulation of stilbene synthase transcripts might be damage-related, because the spread of the fungus is not contained.

Outlook

Our study shows that genetic factors present in the ancestral European wild grape can contain the spread of *N. parvum*. Although a gene-for-gene type of resistance is not expected in this type of disease, it would be rewarding to undertake a comparative screening with different isolates to gain insight into potential strain specificities. Also, other forms of GTDs threatening European viticulture, such as the Esca syndrome, should be considered. In the meantime, the first crossbreeding population

between a representative of the *V. sylvestris* RVC and a *vinifera* variety has been established, screened and sequenced, which allowing the identification of molecular markers, and associated high stilbene inducibility, as a first step in a smart-breeding strategy for Botryosphaeriaceae-related dieback resistance. In addition to this application of our research, our model leads to interesting questions linked to the chemical crosstalk between host and pathogen: the behavioural switch of the fungus, when the host plant is shifted under stress, suggests that the pathogen can sense the status of the host. On the other hand, the observation of excessive lignin deposition in the reaction zone of susceptible hosts indicates that soluble signals secreted by the fungus can repartition the secondary metabolism of the host. Our working model predicts that GTD-related fungi secrete compounds that can modify grapevine immunity. The recent finding that the GTD fungus *Eutypa lata* secretes *O*-methylmellein that can amplify defence responses triggered by the bacterial PAMP flg22 (Guan *et al.*, 2020) suggests that there is still much to be discovered in plant–fungal communication.

Acknowledgements


This work was supported by the European Fund for Regional Development (Interreg Upper Rhine, projects Vitifutur, and DialogProTec), and by a fellowship from the German Egyptian Research Long-term Scholarships DAAD-GERLS programme to IK. Also, the authors acknowledge Hélène Laloue and Mélanie Bénard-Gellon, from Université de Haute-Alsace, Colmar, France, for providing the fungal strain *N. parvum* Bt-67 and


taught IK the infection assay. Open access funding was enabled and organized by Projekt DEAL.


Author contributions

IMK designed the research, conducted all experiments and wrote the manuscript. VPS supervised and reviewed the anatomy (histochemistry and cryo-SEM). RB, AM-G and PH carried out LC-MS (stilbene analysis). EB and MD hosted and supervised cryo-SEM imaging. MR supervised and reviewed the molecular biology. PN conceived the hypothesis-driven research, supervised and commented on the manuscript.

ORCID

Raymonde Baltenweck  <https://orcid.org/0000-0002-8228-1517>


Markus Dürrenberger  <https://orcid.org/0000-0002-4408-7158>

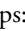
Philippe Hugueney  <https://orcid.org/0000-0002-1641-9274>

Islam M. Khattab  <https://orcid.org/0000-0003-2370-0766>

Alessandra Maia-Grondard  <https://orcid.org/0000-0003-0218-5566>

Peter Nick  <https://orcid.org/0000-0002-0763-4175>

Michael Riemann  <https://orcid.org/0000-0003-0287-2112>

Vaidurya P. Sahi  <https://orcid.org/0000-0003-3814-5953>

References

- Adrian M, Jeandet P. 2012. Effects of resveratrol on the ultrastructure of *Botrytis cinerea* conidia and biological significance in plant/pathogen interactions. *Fitoterapia* 83: 1345–1350.
- Alonso-Villaverde V, Voinesco F, Viret O, Spring JL, Gindro K. 2011. The effectiveness of stilbenes in resistant Vitaceae: ultrastructural and biochemical events during *Plasmopara viticola* infection process. *Plant Physiology and Biochemistry* 49: 265–274.
- Amalfitano C, Evidente A, Surico G, Tegli S, Bertelli E, Mugnai L. 2000. Phenols and stilbene polyphenols in the wood of esca-diseased grapevines. *Phytopathologia Mediterranea* 39: 178–183.
- Arend M, Weisenseel MH, Brummer M, Osswald W, Fromm JH. 2002. Seasonal changes of plasma membrane H⁺-ATPase and endogenous ion current during cambial growth in poplar plants. *Plant Physiology* 129: 1651–1663.
- Arroyo-García R, Ruiz-García L, Bolling L, Ocete R, López MA, Arnold C, Ergul A, Söylemezoğlu G, Uzun HI, Cabello F. *et al.* 2006. Multiple origins of cultivated grapevine (*Vitis vinifera* L. ssp. *sativa*) based on chloroplast DNA polymorphisms. *Molecular Ecology* 15: 3707–3714.
- Bacete L, Mélida H, Miedes E, Molina A. 2018. Plant cell wall-mediated immunity: cell wall changes trigger disease resistance responses. *The Plant Journal* 93: 614–636.
- Barnes W, Anderson C. 2017. Acetyl bromide soluble lignin (ABSL) assay for total lignin quantification from plant biomass. *Bio-Protocol* 7: 1–11.
- Baskarathevan J. 2011. *Botryosphaeriaceous infection in New Zealand vineyards: identification, population structure and genetic diversity*. PhD thesis, Lincoln University, New Zealand.
- Bertsch C, Ramírez-Suero M, Magnin-Robert M, Larignon P, Chong J, Abou-Mansour E, Spagnolo A, Clément C, Fontaine F. 2013. Grapevine trunk diseases: complex and still poorly understood. *Plant Pathology* 62: 243–265.
- Breuil AC, Jeandet P, Adrian M, Chopin F, Pirio N, Meunier P, Bessis R. 1999. Characterization of a pterostilbene dehydrodimer produced by laccase of *Botrytis cinerea*. *Phytopathology* 89: 298–302.
- Coakley SM, Scherm H, Chakraborty S. 1999. Climate change and plant disease management. *Annual Review of Phytopathology* 37: 399–426.
- European Commission. 2009. *Regulation (EC) no 552/2009 of 22 June 2009 amending Regulation (EC) no 1907/2006 of the European Parliament and of the Council on the Registration, Evaluation, Authorisation and Restriction of Chemicals (REACH) as regards annex XVII*. URL <http://data.europa.eu/eli/reg/2009/552/oj>. Brussels, Belgium: European Commission.
- Cota-Sánchez JH, Remarchuk K, Ubayasena K. 2006. Ready-to-use DNA extracted with a CTAB method adapted for herbarium specimens and mucilaginous plant tissue. *Plant Molecular Biology Reporter* 24: 161–167.
- Dai GH, Andary C, Mondolot-Cosson L, Boubals D. 1995. Histochemical studies on the interaction between three species of grapevine, *Vitis vinifera*, *V. rupestris* and *V. rotundifolia* and the downy mildew fungus, *Plasmopara viticola*. *Physiological and Molecular Plant Pathology* 46: 177–188.
- Djoukeng JD, Polli S, Larignon P, Abou-Mansour E. 2009. Identification of phytotoxins from *Botryosphaeria obtusa*, a pathogen of black dead arm disease of grapevine. *European Journal of Plant Pathology* 124: 303–308.
- Duan D, Fischer S, Merz P, Bogs J, Riemann M, Nick P. 2016. An ancestral allele of grapevine transcription factor MYB14 promotes plant defence. *Journal of Experimental Botany* 67: 1795–1804.
- Duan D, Halter D, Baltenweck R, Tisch C, Tröster V, Kortekamp A, Hugueney P, Nick P. 2015. Genetic diversity of stilbene metabolism in *Vitis sylvestris*. *Journal of Experimental Botany* 66: 3243–3257.
- Fontaine F, Gramaje D, Armengol J, Smart R, Nagy ZA, Borgo M, Rego C, Corio-Costet M-F. 2016. *Grapevine trunk diseases. A review*. International Organisation of Vine and Wine (OIV), (December), 25. [WWW document] URL <http://www.oiv.int/public/medias/4650/trunk-diseases-oiv-2016>.
- Gerlach D. 1977. *Botanische Mikrotechnik Eine Einführung*, 2, überarbeitete und erweiterte Auflage. XII + 311 S., 45 Abb. Georg Thieme Verlag. Stuttgart, ISBN 3-13-444902-1. *Feddes Repertorium* 89: 99–100.
- Gómez P, Báidez AG, Ortuño A, Del Río JA. 2016. Grapevine xylem response to fungi involved in trunk diseases. *Annals of Applied Biology* 169: 116–124.
- Guan P, Schmidt F, Riemann M, Fischer J, Thines E, Nick P. 2020. Hunting modulators of plant defence: the grapevine trunk disease fungus *Eutypa lata* secretes an amplifier for plant basal immunity. *Journal of Experimental Botany* 71: 3710–3724.
- Guan X, Essakhi S, Laloue H, Nick P, Bertsch C, Chong J. 2016. Mining new resources for grape resistance against Botryosphaeriaceae: a focus on *Vitis vinifera* subsp. *sylvestris*. *Plant Pathology* 65: 273–284.
- Jiao Y, Xu W, Duan D, Wang Y, Nick P. 2016. A stilbene synthase allele from a Chinese wild grapevine confers resistance to powdery mildew by recruiting salicylic acid signalling for efficient defence. *Journal of Experimental Botany* 67: 5841–5856.
- Jones J, Dangl J. 2006. The plant immune system. *Nature* 444: 323–329.
- Kelloniemi J, Trouvelot S, Heloir M-C, Simon A, Dalmais B, Frettinger P, Cimerman A, Fermaud M, Roudet J, Baulande S *et al.* 2015. Analysis of the molecular dialogue between Gray Mold (*Botrytis cinerea*) and Grapevine (*Vitis vinifera*) reveals a clear shift in defense mechanisms during berry ripening. *Molecular Plant-Microbe Interactions* 28: 1167–1180.
- Keylor MH, Matsuura BS, Stephenson CRJ. 2015. Chemistry and biology of resveratrol-derived natural products. *Chemical Reviews* 115: 8976–9027.
- Kumar SN, Nambisan B. 2014. Antifungal activity of diketopiperazines and stilbenes against plant pathogenic fungi *in vitro*. *Applied Biochemistry and Biotechnology* 172: 741–754.
- Langcake P. 1981. Disease resistance of *Vitis* spp. and the production of the stress metabolites resveratrol, e-viniferin, α-viniferin and pterostilbene. *Physiological Plant Pathology* 18: 213–226.
- Li H, Durbin R. 2010. Fast and accurate long-read alignment with Burrows–Wheeler transform. *Bioinformatics* 26: 589–595.
- Li H, Handsaker B, Wysoker A, Fennell T, Ruan J, Homer N, Marth G, Abecasis G, Durbin R. 2009. The Sequence Alignment/Map format and SAMtools. *Bioinformatics* 25: 2078–2079.
- Liang Z, Duan S, Sheng J, Zhu S, Ni X, Shao J, Liu C, Nick P, Du F, Fan P *et al.* 2019. Whole-genome resequencing of 472 *Vitis* accessions for grapevine diversity and demographic history analyses. *Nature Communications* 10: 1–12.

- Livak KJ, Schmittgen TD. 2001. Analysis of relative gene expression data using real-time quantitative PCR and the $2^{-\Delta\Delta CT}$ method. *Methods* 25: 402–408.
- Massonnet M, Figueroa-Balderas R, Galarneau ERA, Miki S, Lawrence DP, Sun Q, Wallis CM, Baumgartner K, Cantu D. 2017. *Neofusicoccum parvum* colonization of the grapevine woody stem triggers asynchronous host responses at the site of infection and in the leaves. *Frontiers Plant Science* 8. doi: 10.3389/fpls.2017.01117.
- Nick P. 2014. Schützen und nützen – von der Erhaltung zur Anwendung. Fallbeispiel Europäische Wildrebe. *Hoppea Denkschrift* 159–173.
- Parage C, Tavares R, Rety S, Baltenweck-Guyot R, Poutaraud A, Renault L, Heintz D, Lugin R, Marais GAB, Aubourg S *et al.* 2012. Structural, functional, and evolutionary analysis of the unusually large stilbene synthase gene family in grapevine. *Plant Physiology* 160: 1407–1419.
- Paterson AH, Kim C, Guo H, Wang X, Lee T-H. 2014. SNPPhylo: a pipeline to construct a phylogenetic tree from huge SNP data. *BMC Genomics* 15: 162.
- Pezet R, Gindro K, Viret O, Spring JL. 2004. Glycosylation and oxidative dimerization of resveratrol are respectively associated to sensitivity and resistance of grapevine cultivars to downy mildew. *Physiological and Molecular Plant Pathology* 65: 297–303.
- Pierron RJG, Pouzoulet J, Couderc C, Judic E, Compant S, Jacques A. 2016. Variations in early response of grapevine wood depending on wound and inoculation combinations with *Phaeoacremonium aleophilum* and *Phaeoaniella chlamydospora*. *Frontiers in Plant Science* 7: 1–14.
- Pouzoulet J, Jacques A, Besson X, Dayde J, Mailhac N. 2013. Histopathological study of response of *Vitis vinifera* cv. Cabernet Sauvignon to bark and wood injury with and without inoculation by *Phaeoaniella chlamydospora*. *Phytopathologia Mediterranea* 52: 313–323.
- Pouzoulet J, Pivovarov AL, Santiago LS, Rolshausen PE. 2014. Can vessel dimension explain tolerance toward fungal vascular wilt diseases in woody plants? Lessons from Dutch elm disease and esca disease in grapevine. *Frontiers in Plant Science* 5: 1–11.
- Pouzoulet J, Scudiero E, Schiavon M, Rolshausen PE. 2017. Xylem vessel diameter affects the compartmentalization of the vascular pathogen *Phaeoaniella chlamydospora* in grapevine. *Frontiers in Plant Science* 8: 1–13.
- Romanazzi G, Murolo S, Pizzichini L, Nardi S. 2009. Esca in young and mature vineyards, and molecular diagnosis of the associated fungi. *European Journal of Plant Pathology* 125: 277–290.
- Schellenberger R, Touchard M, Clément C, Baillieux F, Cordelier S, Crouzet J, Dorey S. 2019. Apoplastic invasion patterns triggering plant immunity: plasma membrane sensing at the frontline. *Molecular Plant Pathology* 20: 1602–1616.
- Schröder S, Kortekamp A, Heene E, Daumann J, Valea L, Nick P. 2015. Crop wild relatives as genetic resources – the case of the European wild grape. *Canadian Journal of Plant Science* 95: 905–912.
- Slippers B, Wingfield MJ. 2007. Botryosphaeriaceae as endophytes and latent pathogens of woody plants: diversity, ecology and impact. *Fungal Biology Reviews* 21: 90–106.
- Sosnowski MR, Creaser ML, Wicks TJ, Lardner R, Scott ES. 2008. Protection of grapevine pruning wounds from infection by *Eutypa lata*. *Australian Journal of Grape and Wine Research* 14: 134–142.
- Spagnolo A, Mondello V, Larignon P, Villaume S, Rabenoelina F, Clément C, Fontaine F. 2017. Defense responses in grapevine (Cv. Mourvèdre) after inoculation with the Botryosphaeria dieback pathogens *Neofusicoccum parvum* and *Diplodia seriata* and their relationship with flowering. *International Journal of Molecular Sciences* 18: 1–12.
- Stael S, Kmiecik P, Willems P, Van Der Kelen K, Coll NS, Teige M, Van Breusegem F. 2015. Plant innate immunity - sunny side up? *Trends in Plant Science* 20: 3–11.
- Stempien E, Goddard ML, Wilhelm K, Tarnus C, Bertsch C, Chong J. 2017. Grapevine Botryosphaeria dieback fungi have specific aggressiveness factor repertory involved in wood decay and stilbene metabolization. *PLoS ONE* 12: 1–22.
- Svyatyna K, Kikumaru Y, Brendel R, Reichelt M, Mithöfer A, Takano M, Kamiya Y, Nick P, Riemann M. 2014. Light induces jasmonate-isoleucine conjugation via OsJAR1-dependent and -independent pathways in rice. *Plant, Cell & Environment* 37: 827–839.
- Tassoni A, Fornalè S, Franceschetti M, Musiani F, Michael AJ, Perry B, Bagni N. 2005. Jasmonates and Na-orthovanadate promote resveratrol production in *Vitis vinifera* cv. Barbera cell cultures. *New Phytologist* 166: 895–905.
- Úrbez-Torres JR. 2011. The status of Botryosphaeriaceae species infecting grapevines José. *Phytopathologia Mediterranea* 50.
- Úrbez-Torres JR, Haag P, Bowen P, O’Gorman DT. 2013. Grapevine trunk diseases in British Columbia: incidence and characterization of the fungal pathogens associated with black foot disease of grapevine. *Plant Disease* 98: 456–468.
- Vannozzi A, Dry IB, Fasoli M, Zenoni S, Lucchin M. 2012. Genome-wide analysis of the grapevine stilbene synthase multigenic family: genomic organization and expression profiles upon biotic and abiotic stresses. *BMC Plant Biology* 12: doi: 10.1186/1471-2229-12-130.
- Wagschal I, Abou-Mansour E, Petit A-N, Clément C, Fontaine F. 2008. Wood diseases of grapevine: A review on eutypa dieback and esca. In: Barka EA, Clément C, eds. *Plant-microbe interactions*. Kerala, India: Research Signpost, 37, 661–686.
- Walker SE, Lorsch. 2013. RNA purification – Precipitation methods. In: Lorsch J, ed. *Laboratory methods in enzymology: RNA. Methods in enzymology*. New York, NY, USA: Academic Press Inc., 530, 337–343.
- Wang L, Sadeghnezhad E, Riemann M, Nick P. 2019. Microtubule dynamics modulate sensing during cold acclimation in grapevine suspension cells. *Plant Science* 280: 18–30.

Supporting Information

Additional Supporting Information may be found online in the Supporting Information section at the end of the article.

Fig. S1 Heat map of metabolite abundance under different sets; control, wounding and infection in both the piceid chemotype and resveratrol–viniferin chemotype.

Fig. S2 Fungal DNA abundance in the resistant model (Ke15) and susceptible model (Ke94).

Fig. S3 Genotypic differences in lignin and pectin metabolism using histochemical labelling.

Fig. S4 Steady-state transcript levels for three stilbene synthases in response to exogenous methyl jasmonate.

Fig. S5 Genotypic differences in relative cross-section area of pith parenchyma and stem cross-section area.

Methods S1 Fungal DNA detection at infected wood.

Table S1 Genetic details and the primer sequences of the targeted genes.

Please note: Wiley Blackwell are not responsible for the content or functionality of any Supporting Information supplied by the authors. Any queries (other than missing material) should be directed to the *New Phytologist* Central Office.